

Computerized interferometric measurement of surface microstructure

James C. Wyant

WYKO Corporation, 2650 E. Elvira Road
Tucson, Arizona 85706, U.S.A.

&

Optical Sciences Center
University of Arizona
Tucson, Arizona 85721, U.S.A.

ABSTRACT

Nearly all modern high-quality measuring instruments now use micro computers for the collection and analysis of data. This paper describes a computerized interferometric microscope system for the measurement of surface microstructure. For the instrument described in this paper the surface microstructure can be measured at data array sizes as large as 739 x 484 points for measurement fields ranging from 30 x 25 microns to 8.2 x 6.1 mm. A repeatability of the surface height measurements of less than 0.1 nm can be obtained for smooth surfaces. Surfaces having height variations as large as 500 microns can be measured to within an accuracy of a few nanometers.

Keywords: Interferometry, metrology, non-contact profiling, microstructure.

1. INTRODUCTION

Figure 1 shows a simplified schematic of the instrument (called RST Plus).¹⁻³ The configuration shown in Figure 1 utilizes a two-beam Mirau interferometer at the microscope objective. A tungsten halogen lamp is used as the light source. In the phase shifting mode of operation, described below, a spectral filter of 40 nm bandwidth centered at 650 nm is used to increase the coherence length. For the vertical scanning mode of operation, also described below, the spectral filter is not used. Light reflected from the test surface interferes with light reflected from the reference. The resulting interference pattern is imaged onto the CCD array. The output of the CCD array can be viewed on the TV monitor. Also, output from the CCD array is digitized and read by the computer. The Mirau interferometer is mounted on either a piezoelectric transducer (PZT) or a motorized stage so that it can be moved. During this movement, the distance from the lens to the reference surface remains fixed. Thus, a phase shift is introduced into one arm of the interferometer. By introducing a phase shift into only one arm while recording the interference pattern that is produced, it is possible to perform either the direct phase measurement technique described below or the vertical scanning coherence sensing technique also described below. The complete RST Plus system includes a Pentium computer running Microsoft Windows for data analysis and graphics display.

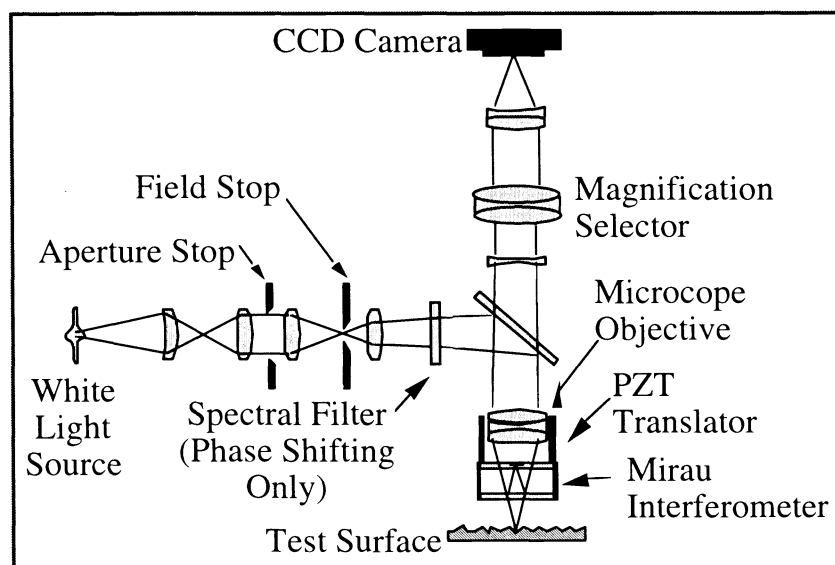


Figure 1. Optical schematic of interference microscope used for measurement of fine surface structure.

Data analysis of the surface profile provides the peak-to-valley roughness of the surface, the root-mean-square roughness (R_q), the arithmetic mean (R_a), and the peak-to-valley height (R_t). The output is in the form of color contour maps, three-dimensional surface plots, slices through the three-dimensional plots, histograms, and bearing ratio plots. If the operator desires, the computer analysis can also provide output describing slope maps, power spectra, autocovariance, peak distribution, and zero crossings. The software has the capability to frequency filter the data.

The Mirau interferometer is used with magnification objectives of 40X, 20X, and 10X. 2.5X and 1.5X magnifications are also available using a Michelson interferometer. A large numerical aperture 100X magnification can be achieved using a Linnik interferometer. Table 1 shows the specifications for the different magnifications available. For additional variations of the field of view, a magnification selector placed between the microscope objective and the CCD array can change the overall magnification by 0.5 or 2.0X.

Two modes of operation are available. For smooth surfaces the phase shifting mode is used since it gives sub-nanometer height resolution capability. For rougher surfaces, up to several hundred micron surface height variations, a vertical scanning coherence sensing technique is used which gives approximately a 3 nm height resolution. These two modes of operation are described below.

2. PHASE-SHIFTING INTERFEROMETRY

An optical profiler can use several phase measurement techniques that yield more accurate height measurements than are possible with the traditional technique, which determines visually how much

interference fringes depart from being straight and equally spaced. One mode of operation of the profiler described in this paper is the integrated-bucket phase shifting technique.⁴⁻⁵

For this technique, the phase difference between the interfering beams is changed at a constant rate as the detector is read out. Each time the detector array is read out, the time variable phase, $\alpha(t)$, has changed by 90° for each pixel. The basic equation for the irradiance of a two-beam interference pattern is given by

$$I = I_1 + I_2 \cos[\phi(x,y) + \alpha(t)] \quad (1)$$

where the first term is the average irradiance, the second term is the interference term, and $\phi(x,y)$ is the phase distribution being measured. If the irradiance is integrated while $\alpha(t)$ varies from 0 to $\pi/2$, $\pi/2$ to π , and π to $3\pi/2$, the resulting signals at each detected point are given by

$$\begin{aligned} A(x,y) &= I_1' + I_2' [\cos \phi(x,y) - \sin \phi(x,y)] \\ B(x,y) &= I_1' + I_2' [-\cos \phi(x,y) - \sin \phi(x,y)] \\ C(x,y) &= I_1' + I_2' [-\cos \phi(x,y) + \sin \phi(x,y)]. \end{aligned} \quad (2)$$

From the values of A, B, and C, the phase can be calculated as

$$\phi(x,y) = \tan^{-1} [(C(x,y) - B(x,y)) / (A(x,y) - B(x,y))]. \quad (3)$$

The subtraction and division cancel out the effects of fixed pattern noise and gain variations across the detector, as long as the effects are not so large that the dynamic range of the detector becomes too small to be of use.

Because Eq. (3) gives the phase modulo 2π , there may be discontinuities present in the calculated phase. These 2π discontinuities can be removed as long as the slopes on the sample being measured are limited so that the actual phase difference between adjacent pixels is less than π . This is done by adding or subtracting multiples of 2π to a pixel until the difference between it and its adjacent pixel is less than π .

Once the phase $\phi(x,y)$ is determined across the interference field, the corresponding height distribution $h(x,y)$ on the test surface is determined by the equation

$$h(x,y) = (\lambda/4\pi) \phi(x,y). \quad (4)$$

3. VERTICAL SCANNING COHERENCE SENSING

In the vertical scanning coherence sensing mode of operation an unfiltered white light source is used. Due to the large spectral bandwidth of the source, the coherence length of the source is short, and good

contrast fringes will be obtained only when the two paths of the interferometer are closely matched in length. Thus, if in the interference microscope the path length of the sample arm of the interferometer is varied, the height variations across the sample can be determined by looking at the sample position for which the fringe contrast is a maximum. In this measurement there are no height ambiguities and, since in a properly adjusted interferometer the sample is in focus when the maximum fringe contrast is obtained, there are no focus errors in the measurement of surface microstructure.⁶⁻⁹

The major drawback of this type of scanning interferometer measurement is that only a single surface height is being measured at a time and a large number of measurements and calculations are required to determine a large range of surface height values. One method for processing the data that gives both fast and accurate measurement results is to use conventional communication theory and digital signal processing (DSP) hardware to demodulate the envelope of the fringe signal to determine the peak of the fringe contrast.^{8,9} Vertical scan rates as large as 7.2 microns per second are available.

Figure 2 shows the irradiance at a single sample point as the sample is translated through focus. It should be noted that this signal looks a lot like an amplitude modulated (AM) communication signal. To obtain the location of the peak, and hence the surface height information, this irradiance signal is detected using a CCD array. The signal is sampled at fixed intervals, such as every 50 to 100 nm, as the sample path is varied. The motion can be accomplished using a piezoelectric transducer. Low frequency and DC signal components are removed from the signal by digital highpass filtering. The signal is next rectified by square-law detection and digitally lowpass filtered. The peak of the lowpass filter output is located and the vertical position corresponding to the peak is noted. Interpolation between sample points can be used to increase the resolution of the instrument beyond the sampling interval. This type of measurement system produces fast, non-contact, true three-dimensional area measurements for both large steps and rough surfaces.

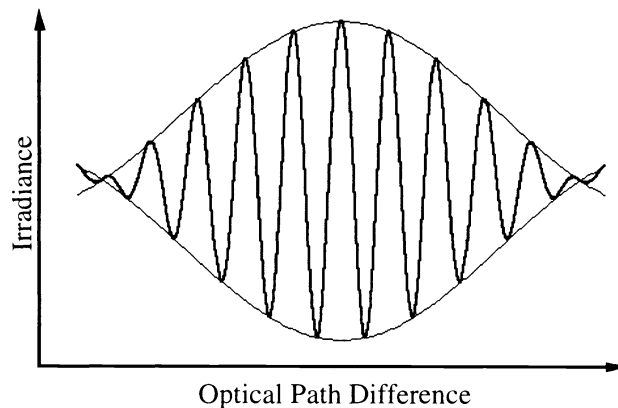


Figure 2. Irradiance at a single sample point as the sample is translated through focus.

4. FIELD OF VIEW, SPATIAL SAMPLING INTERVAL, AND SURFACE SLOPE LIMIT

Table 1 gives the field of view, spatial sampling interval, and surface slope limit for the different objectives and magnification selector used between the objective lens and the CCD array. Other magnifications could be used, but these are typical magnifications used in interference microscopes.

Table 1. Field of View, Sampling Interval, and Slope Limit.

Magnification objective	1.5X	2.5X	10X	20X	40X	100X
Interferometer type	Michelson	Michelson	Mirau	Mirau	Mirau	Linnik
Numerical aperture	0.036	0.075	0.25	0.4	0.5	0.9
Working distance (mm)	18	2	4	1.9	3.9	0.2
Field of view (mm) (with magnification selector)						
0.5X	8.2 x 6.1	4.9 x 3.7	1.2 x 0.9	0.6 x 0.5	0.3 x 0.2	0.12 x 0.09
1.0X	4.3 x 3.2	2.6 x 1.9	0.6 x 0.5	0.3 x 0.2	0.15 x 0.1	0.06 x 0.05
2.0X	2.1 x 1.6	1.3 x 1.0	0.3 x 0.2	0.2 x 0.1	0.08 x 0.06	0.03 x 0.02
Spatial sampling (with magnification selector) (micron)						
0.5X	12.7	7.6	1.9	1	0.5	0.2
1.0X	6.6	4	1	0.5	0.2	0.1
2.0X	3.3	2	0.5	0.2	0.1	0.05

5. MEASUREMENT EXAMPLES

The applications for an interferometer for the measurement of fine structure are diverse, ranging from optical surfaces, to magnetic media and thin film read/write heads, to machined surfaces, to biomedical applications, to almost any surface imagined. Some examples of measurements of various surfaces are shown in Figures 3 through 6 in three-dimensional plotted format. Other display formats are available including color contour maps, two-dimensional plots, histograms and various data analyses which do not reproduce well in black and white.

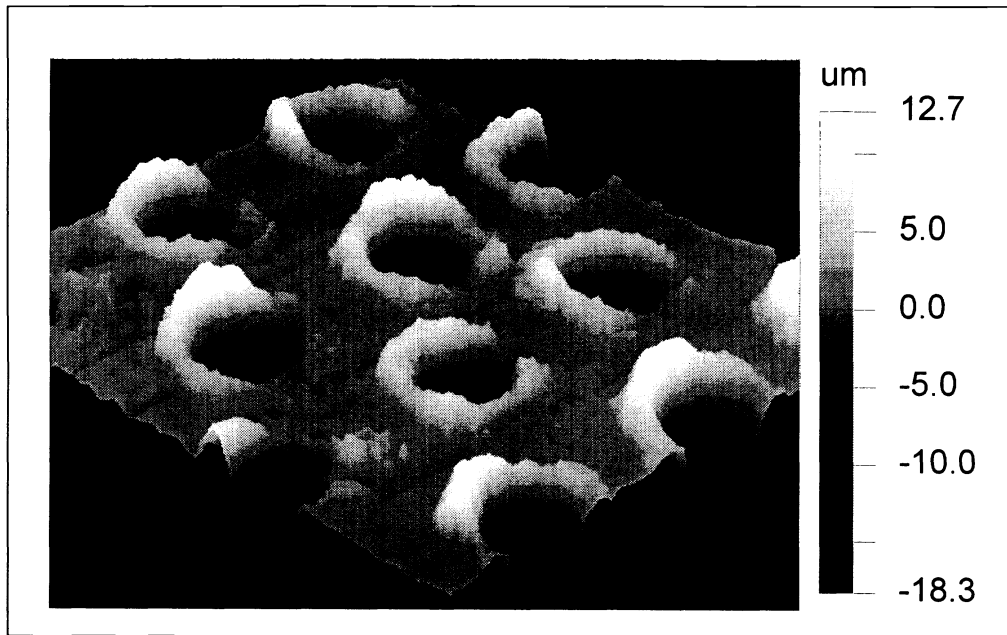


Figure 3. Three-dimensional plot of metal plate with laser drilled holes having $R_q=5.07$ microns, $R_a=3.44$ microns, and $R_t=31.05$ microns.

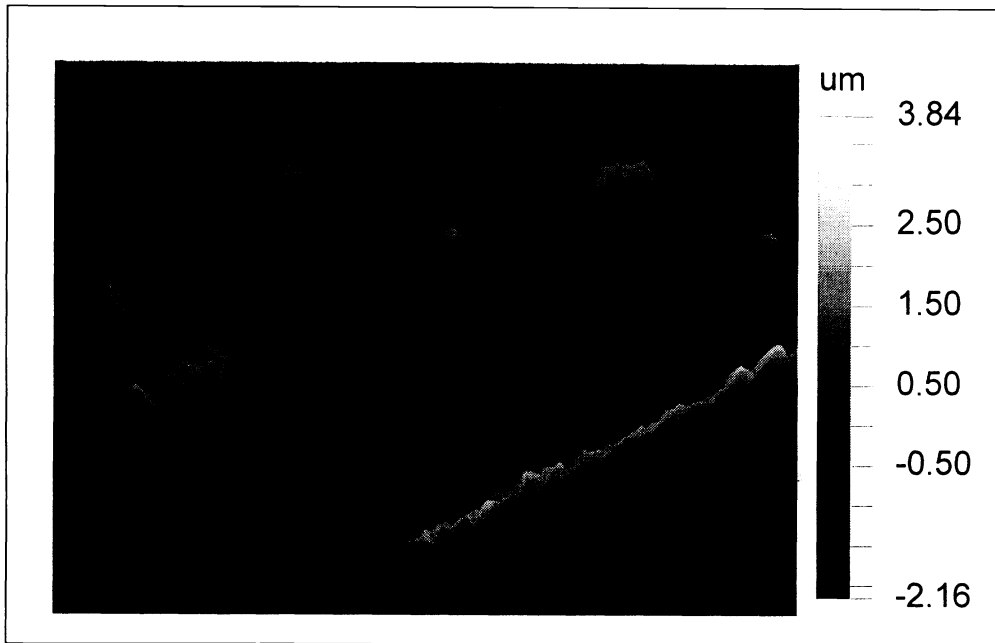


Figure 4. Three-dimensional surface map of camshaft showing tool chatter having $R_q=790.4$ nm, $R_a=626.51$ nm, and $R_t=6.00$ microns.

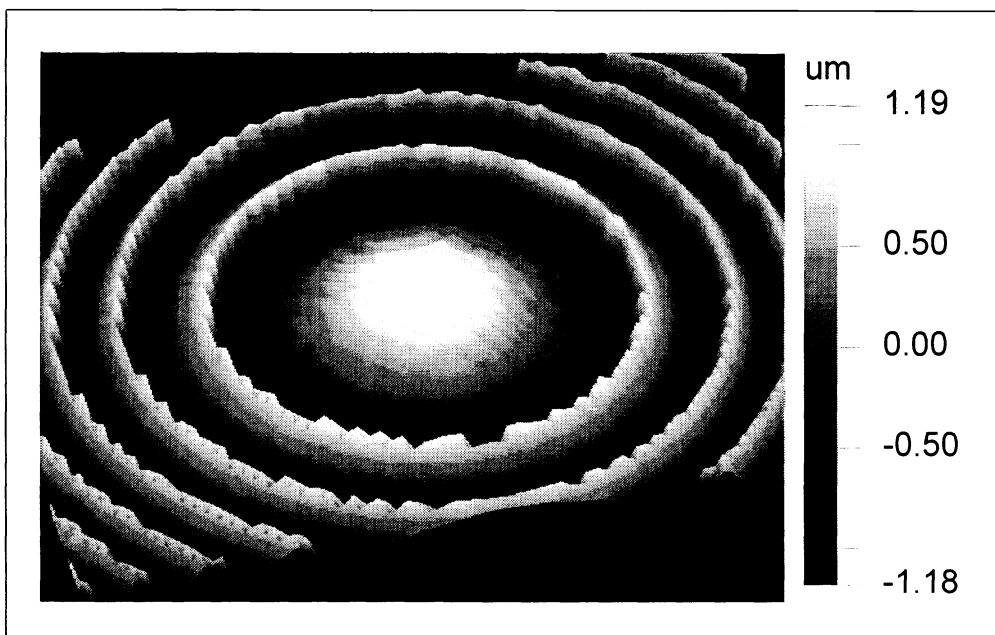


Figure 5. Three-dimensional surface map of binary lens having $R_q=561.30$ nm, $R_a=476.71$ nm, and $R_t=2.37$ microns.

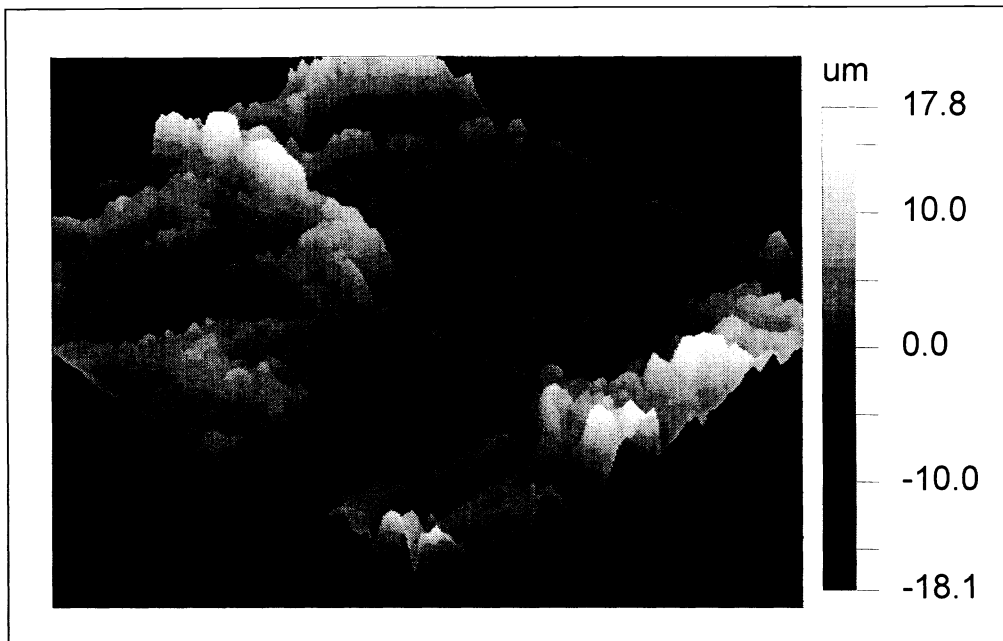


Figure 6. Three-dimensional surface map of paper sample having Rq=4.91 microns, Ra=3.89 microns, and Rt=35.85 microns.

CONCLUSION

This paper has described the operation and performance of a non-contact microsurface profiling instrument. This computer-controlled instrument has extensive software and, while it is only possible to illustrate a few of the profile results here, it has been demonstrated to provide useful surface data for a wide variety of surfaces. The instrument has found extensive uses in applications such as the testing of optical components and the evaluation of the recording heads used in magnetic disk drives in computers. The instrument is used in measuring the print rollers used in the printing industry and measuring gears and bearings for the automotive industry. In the biomedical area the instrument is useful for measuring heart valves and hip joint replacements. The microscope is even useful in exotic applications such as measuring potato chip bags to determine which ones are most likely to keep the potato chips fresh for the longest time.

REFERENCES

1. B. Bhushan, J.C. Wyant and C.L. Koliopoulos, "Measurement of surface topography of magnetic tapes by Mirau interferometry," *Appl. Opt.*, 28, 1489-1497, 1985.
2. J.C. Wyant, "Optical profilers for surface roughness," *Proc. SPIE*, 525, 174-180, 1985.
3. J. C. Wyant and K. Creath, "Advances in interferometric optical profiling," *Int. J. Mach. Tools Manufact.*, 32(1/2), 5-10, 1992.
4. J. C. Wyant, "Use of an ac heterodyne lateral shear interferometer with real-time wavefront corrections systems," *Appl. Opt.*, 14(11), 2622-2626, Nov. 1975.
5. K. Creath, "Phase-shifting interferometry techniques," in *Progress in Optics XXVI*, E. Wolf, ed. (Elsevier Science, 1988), pp. 357-373.
6. M. Davidson, K. Kaufman, I. Mazor, and F. Cohen, "An application of interference microscopy to integrated circuit inspection and metrology," *Proc. SPIE*, 775, 233-247 (1987).
7. G. S. Kino and S. Chim, "Mirau correlation microscope," *Appl. Opt.* 29, 3775-3783 (1990).
8. T. Dresel, G. Hausler, and H. Venzke, "Three-dimensional sensing of rough surfaces by coherence radar," *Appl. Opt.* 31(7), 919-925, March 1992.
9. P. J. Caber, "An interferometric profiler for rough surfaces," *Appl. Opt.* 32(19), 3438-3441, July 1993.